RSC Advances

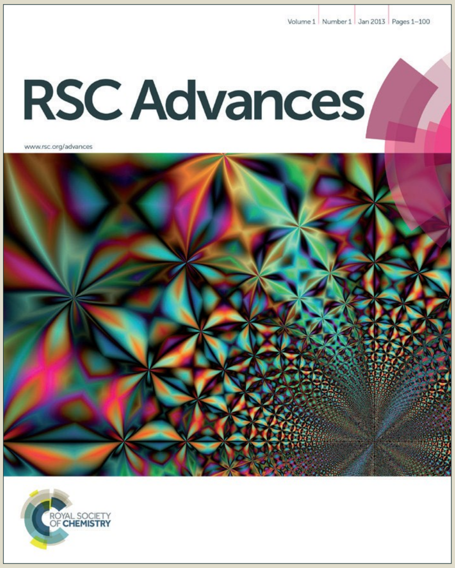

ROYAL SOCIETY OF CHEMISTRY

www.rsc.org/advances

Journal Name

ARTICLE

ZrO_2/SBA-15 as an efficient catalyst for the production of γ-valerolactone from biomass derived levulinic acid in vapour phase at atmospheric pressure

Received 00th January 20xx,
Accepted 00th January 20xx

DOI: 10.1039/x0xx00000x

www.rsc.org/

Enumula Siva Sankar, G.V. Ramesh Babu, Kondeboina Murali, Burri David Raju, and Kamaraju Seetha Rama Rao*

γ-valerolactone is a promising renewable feedstock for the production of fuels and industrial chemicals. In this work, SBA-15 supported ZrO_2 catalysts prepared by wet impregnation method with various ZrO_2 loadings ranging from 10 to 30 weight % have been studied for the production of γ-valerolactone from levulinic acid via catalytic transfer hydrogenation and cyclization with isopropanol as H-donor in vapour phase at atmospheric pressure. Among the catalysts, 25 weight % ZrO_2 /SBA-15 has been identified as an efficient catalyst for the transfer hydrogenation delivering 100% conversion of levulinic acid with 93% selectivity towards γ-valerolactone. The physicochemical characteristics of these catalysts were achieved by X-ray diffraction, BET surface area, pore size distribution, UV-Visible spectroscopy, Temperature programmed desorption of ammonia, SEM, TEM and ICP-OES techniques. The characterization studies divulge the presence of ZrO_2 with well dispersed acidic sites, enhanced surface area, and ease of accessibility for the active sites within the uniform pore channels, engendered the excellent catalytic performance with low molar ratios 1:7 (levulinic acid: isopropanol). Moreover, the catalyst showed sturdiness during 20 hours time on stream study.

Keywords:Levulinicacid, γ-valerolactone, Catalytic transfer hydrogenation, ZrO_2 /SBA-15

1. Introduction

Currently the World is revolving around the sustainable development of energy sources. This is because of fast declining of fossil fuels which is a serious threat to continuous supply of energy demands of the future generations. In this context, utilization of cellulosic biomass as a renewable precursor for the sustainable production of fuels and commodity chemicals can be regarded as one of the approaches to overcome the problems[1-5]. Cellulosic biomass contains biopolymeric species such as cellulose, hemicelluloses, and lignin. Among these, acidic hydrolysis of cellulose and hemicelluloses produces levulinic acid (LA) as one of the product[6]. LA has been identified as one of the most sustainable top 12 platform chemicals that can be derived from biomass. LA is a versatile molecule (4-oxopentanoic acid) with two reactive functional groups, keto and carboxylic acid groups offering potential applications in the synthesis of value added chemicals like diphenolic acid (DPA, widely used in polymer resin and textile industries), 5-aminolevulinic acid (DALA, used as a defoliant and active ingredient in synthesis of herbicides), pyrrolidines (in pharmaceutical industry) 2-Methyl-3-indoleacetic acid (plant growth hormone). The derivates of LA find applications in various areas such as angelica lactones (perfume and food additive), calcium levulinate (as calcium supplement), levulinate potash (as effective fertilizer). Besides these, LA can be regarded as a promising feedstock for the production of fuels and fuel additives. The esterification products of LA serve as fuel additives. The hydrogenation of LA produces products like γ-valerolactone (GVL), 2-methyl tetrahydro furan, 1,4-pentanediol, valeric acid (regarded as biofuels) etc[7]. R&D efforts are going on the hydrogenation of LA to GVL owing to the ample applications of GVL as a green solvent, food additive, intermediate in the fine chemicals synthesis, in perfume industry, apart from its applications as a renewable, safe, transportable liquid fuel. Recent studies on lighting properties of GVL in combination with ethanol (90/10 v/v %) were shown fruitful results for the usage of GVL as sustainable liquid fuel[8]. The catalytic upgrading of GVL to fuels or carbon based consumer products has shown industrial importance. GVL can be converted into hydrocarbon fuels in multiple steps involving hydrogenation, deoxygenation, decorboxylation, C-C bond formations etc. The successive catalytic conversion of

---

Corresponding author: Inorganic and Physical Chemistry Division, CSIR-Indian Institute of Chemical Technology, Hyderabad, India-5000071. E-mail: ksramarao@iict.res.in & ksramarao.iict@gov.in

† Footnotes relating to the title and/or authors should appear here.

Electronic Supplementary Information (ESI) available: [details of any supplementary information available should be included here]. See DOI: 10.1039/x0xx00000x

GVL produces butene isomers which on further oligomerization lead to form C12 jet fuel. The pentanoic acid obtained through ring opening of GVL would be upgraded to C9-alkanes or C18-alkanes. GVL can be considered as a feedstock for polymer industry. The ring opening products of GVL like methylpentenoates, γ-hydroxy-amides are green polymer precursors[9]. In general GVL has been produced by the hydrogenation and subsequent lactonization of LA or its esters by using either molecular H_2 or Hydrogen-donors (formic acid, secondary alcohols, formate salts). Several homogeneous catalysts were reported for the hydrogenation of LA especially Ru based catalysts yielded good conversions of LA and selectivity's to GVL. However, the major complications associated with these catalysts are catalyst separation, catalyst preparation, and recycling of the used catalyst. The hydrogenation of LA has been performed over various heterogeneous catalysts using molecular H_2 or formic acid as H-donor. Supported metal catalysts were found to be active for the hydrogenation of LA due to the dispersion of metal nano particles and their interaction with the support. A number of supported metal catalysts such as carbon supported noble metal (Ru, Pt, Pd, Au and Rh) catalysts, noble metal catalysts with conventional supports SiO_2, Al_2O_3, ZrO_2, TiO_2, mesoporous silica supported catalysts Pd/MCM-41, and supported non-noble metal catalysts (Cu/SiO_2, Cu/ZrO_2, Ni/TiO_2, Ni-MoO_x/C) were optimized for the hydrogenation of LA to GVL with inspiring activities[9-10]. Most of these hydrogenations need expensive metals (Ru, Pt, Pd, Au and Rh) to facilitate hydrogenation or to decompose formic acid (creating economical and environmental issues), harsh reaction conditions, usage of molecular H_2, and high pressure operations. Thus, there is a need to develop cost effective catalytic processes. An alternative sustainable approach for the production of GVL is catalytic transfer hydrogenation (CTH) of LA or its esters using secondary alcohols as hydrogen donors (Meerwein–Ponndorf–Verley reduction (MPV))[11]. The driving force for the reaction is the alcohol (4-hydroxy pentanoic acid) formed from LA readily lactonizes to GVL, it drives the oxidation of secondary alcohols[12]. Unlike aforementioned hydrogenations the use of inexpensive metal oxides and recovery of secondary alcohols as ketones make this process as sustainable for the production of GVL. Recently, several workers have been explored the synthesis of GVL using MPV reduction. Number of metal oxides and metal hydroxides were tested for the CTH of LA and its esters. Dumesic et.al performed the CTH reaction with ZrO_2 at elevated pressure yielding interesting results[13]. Xing Tang et.al have been reported the conversion of ethyl levulinate (EL) to GVL over ZrO_2 in supercritical ethanol with good conversions. Zr-beta zeolite, Zr-HBA, zirconium hydroxides were also found to be active in GVL production[14-17]. Apart from zirconium based catalysts, Ni catalysts could be served as a CTH catalyst in the production of GVL at mild reaction conditions[18]. The literature study reveals that zirconium based catalysts are active in catalyzing CTH of several carbonyl compounds in batch and continuous process at mild reaction conditions[19-20]. However, their applicability is limited due to their limited surface areas and pore sizes. In recent years, mesoporous silica materials have attracted the catalysis community because of its unique properties like larger surface areas, uniform tunable pore sizes, diffusion limitations, and high thermal stability[21-22]. In our previous work, aiming for synthesis of alkyl levulinates, the formation of GVL was found at the expense of ester in esterification of LA with isopropanol over ZrO_2/SBA-15 catalyst[23]. Hence, it can be expected that the dispersion of ZrO_2 on SBA-15 could enhance its catalytic performance in CTH reaction by increasing the accessibility of the reactants on the dispersed acidic sites over larger surface areas within the uniform pore channels. In this context, we have prepared ZrO_2/SBA-15 catalysts with different loadings of zirconia by means of wet impregnation method. Several characterization techniques have been used to know the physicochemical characteristics of the prepared catalysts, namely X-ray diffraction (XRD), BET surface area, pore size distribution, UV-Visible spectroscopy, NH_3-TPD, SEM, TEM and ICP-OES techniques. The catalytic studies of ZrO_2/SBA-15 catalysts for CTH of levulinic acid were conducted in a fixed bed reactor, at atmospheric pressure. Various reaction parameters like reaction temperature, ZrO_2 loading, molar ratios of LA to isopropanol, time on stream study and effect of different secondary alcohols and substrates were studied. Special attention was paid on catalyst stability and reusability.

2. Experimental

2.1 Catalyst preparation

SBA-15 mesoporous silica was prepared according to the literature described elsewhere[21-22]. In a typical synthesis, a solution containing a composition of P123:2MHCl:TEOS: H_2O = 2:60:4.25: 15 (mass ratio) was prepared, stirred at 40 °C for 24 h, followed by hydrothermal treatment at 100 °C for 24 h under static conditions. Then it was filtered and dried in an air oven at 80 °C for 12h. The dried solid was calcined in air flow at 550 °C for 8 h. The resultant mesoporous silica (SBA-15) was used as support. ZrO_2/SBA-15 catalysts with various loadings (10, 15, 20, 25, 30 weight percentages of ZrO_2) were prepared by wet impregnation method with zirconium acetyl acetonate as zirconia precursor. Briefly, requisite amount of the precursor dissolved in methanol was added to the SBA-15 and the mixture was dried with occasional stirring on a hot plate to complete dryness. The solid was dried in an air oven at 100 °C for 12 h, and then calcined at 450 °C for 5 h in static air. The prepared catalyst was labelled as XZS where X represents the weight percentage of ZrO_2. For comparison purpose, commercial ZrO_2 (M/s. Loba chemie, India) was used.

2.2 Characterization of catalysts

The powder X-ray diffraction patterns were recorded on Ultima IV diffractometer (M/s. Rigaku Corporation, Japan) using Ni filtered Cu Kα radiation (λ=1.54178 Å) at 40 kV and 30 mA. The textural parameters were determined by N_2 adsorption–desorption experiments, performed at liquid N_2 temperature on a Quadrasorb-SI (M/s. Quantachrome Instruments Corporation, USA) adsorption unit. Prior to the measurement, the sample was degassed at 150 °C for 2 h. The UV–Vis spectra of the samples were recorded on a UV-2000, (M/s Shimadzu, Japan) spectrophotometer equipped with a diffuse reflectance attachment with an integrating sphere containing $BaSO_4$ as a reference. The distribution of acid sites was probed by the temperature programmed desorption of ammonia. Approximately, 50 mg of catalyst sample loaded in a tubular sample tube was pre-treated in a flow of helium at 300 °C for 30 min. Subsequently, the catalyst sample was saturated with 10% NH_3/He at 80 °C for 30 min. After the saturation, helium was allowed to flow for 30 min at 100 °C for complete removal of physisorbed ammonia. Helium flow was continued while increasing the temperature to 800 °C at a ramp of 10 °C min^{-1} and the desorbed NH_3 was monitored with on-line connected TCD equipped GC using standard GC software. The morphological studies of catalysts were carried out by scanning electron microscope (M/s. JEOL, Switzerland) and TEM images were obtained on a JEM 2000EXII apparatus (M/s. JEOL, Switzerland) operating between 160 and 180 kV respectively. Prior to TEM analysis, the catalyst sample was ultrasonicated in ethanol and a drop was placed onto a carbon coated copper grid, the solvent was then evaporated in an air oven at 80 °C for 6 hours. The composition of ZrO_2 was calculated by means of ICP-OES (M/s. Thermo Scientific iCAP6500 DU) by dissolving the compounds in the aquaregia along with few drops of hydrofluoric acid to digest the SBA-15.

2.3 Catalytic activity

The catalytic tests were performed in fixed-bed quartz down flow reactor (14 mm id and 300 mm length) at atmospheric pressure. For each catalytic run, the reactor was loaded with 0.5 g of the catalyst mixed with same amount of quartz particles sandwiched between two quartz wool plugs at the middle of the reactor. Prior to catalytic test, the catalyst was flushed in N_2 flow (30 ml/min) at 250 °C for 1 h. The liquid feed with required molar ratio (LA: IPA) was fed at a flow rate of 1ml/h using a syringe feed pump (M/s. B. Braun, Germany). The product mixture was collected in an ice cooled trap at regular intervals and analyzed by a FID equipped GC-17A (M/s. Shimadzu Instruments, Japan) with EB–5 capillary column (30 m x 0.53 mm x 5.0 µm) and confirmed by GC-MS, QP-2010 (M/s. Shimadzu Instruments, Japan) with EB–5MS capillary column (30 m x 0.25 mm x 0.25 µm).

3. Results and Discussion

The powder XRD patterns of the catalysts were presented in Figure. 1. From low angle XRD patterns, it is found that the parent SBA-15 and ZrO_2/SBA-15 catalysts have retained their 2D hexagonal pore arrangement, by exhibiting three diffraction peaks at 2θ values of 0.90, 1.60, and 1.80 corresponding to the (100), (110) and (200) reflections respectively, of regular mesoporous 2D hexagonal pore (p6mm) structure[21-24]. The d_{100} and unit cell parameter values shown in Table.1, indicates the intactness of the ordered mesoporous structure even after highest ZrO_2 loading (30 wt %). The shifting of (100) plane of ordered mesoporous SBA-15 in the low angle XRD patterns (Figure.1) of ZrO_2/SBA-15 samples to slightly higher 2θ values compared to that of SBA-15 is due to the coating of inner walls of SBA-15 by oxide monolyaer[25]. Wide angle XRD (Figure. 1. Inset) of the ZrO_2/SBA-15 catalysts show no signals due to the crystalline phase of ZrO_2 up to 15ZS catalyst (15 wt % of zirconia). Beyond 15% ZrO_2 loading, low intense diffraction signals due to tetragonal ZrO_2 phase (ICDD No. 88-1007) were observed. This is a clear indication that, ZrO_2 might be in amorphous form or highly dispersed form (below 4 nm size which is the detection limit of XRD) up to 15**%** ZrO_2 loading, beyond which ZrO_2 crystallites appear with average sizes 8.9, 10.9, and 13.5 nm for 20ZS, 25ZS and 30ZS catalysts respectively. It gives a scope to think at higher ZrO_2 loading, ZrO_2 particles (particle sizes > 5 nm) to reside outside the pores of SBA-15[26]. However one should not forget that saturation of SBA-15 pores with ZrO_2 particles occurs at 15% ZrO_2 loading.

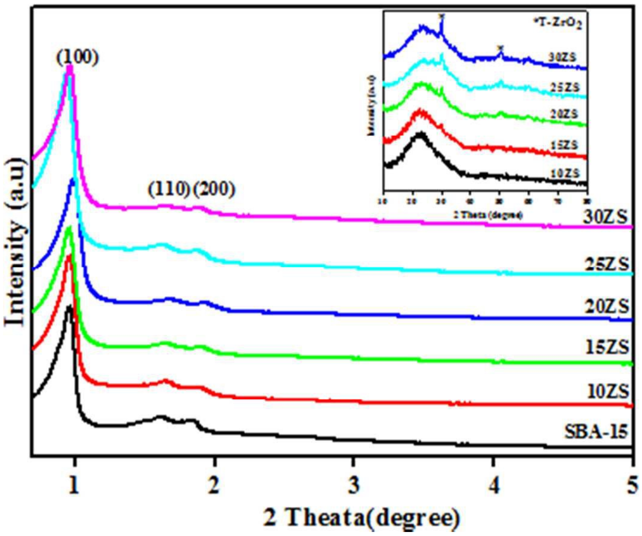

Fig. 1. Low angle XRD pattern of parent SBA-15 and ZrO_2/ SBA-15 and in inset figure wide angle XRD patterns of ZrO_2/SBA-15

At higher loadings, there is every chance for ZrO_2 particles with sizes less than 5 nm to present inside the pore channels of SBA-15 and particles with sizes above 5 nm to present outside the pore channels of SBA-15. Zirconia content in the catalysts was confirmed by the ICP-OES analysis and the values presented in Table.2 are concomitant with the theoretical values.

The N_2-adsorption desorption isotherms and pore size distributions for SBA-15 and ZrO_2/SBA-15 catalysts were depicted in Figure. 2.

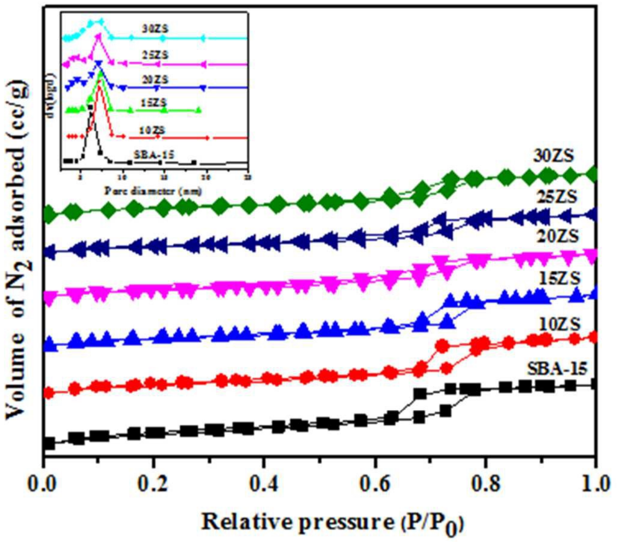

Fig. 2. N_2 adsorption-desorption isotherms for parent SBA-15 and various ZrO_2/SBA-15 samples and in inset figure pore size distribution of parent SBA-15 and ZrO_2/SBA-15 samples

All of them exhibited typical type IV isotherm with H1 hysteresis loop corresponding to IUPAC classification of porous materials, indicating regular mesoporous materials with cylindrical pores. For all the catalysts, capillary condensation was observed within the P/P_0 range ~ 0.6-0.8 which is a characteristic feature for mesoporous solids with highly ordered pores, designating the evenness of the ordered structure even after ZrO_2 deposition[21-24,27].

Table.1 Physico-chemical characteristics of ZrO_2/SBA-15 catalysts

Catalyst	S_{BET}^{a} ($m^2 g^{-1}$)	V_t^{b} (cc/g)	D^c (nm)	$d_{(100)}^{d}$ (nm)	a_0^{e} (nm)	t^f (nm)
SBA-15	703	0.96	5.50	9.32	10.76	5.25
10ZS	558	0.88	6.30	9.20	10.63	4.32
15ZS	514	0.81	6.30	9.25	10.69	4.38
20ZS	474	0.67	5.82	8.90	10.28	4.45
25ZS	446	0.65	5.89	9.32	10.76	4.87
30ZS	429	0.61	5.71	9.20	10.63	4.91
ZrO_2	32	0.08	8.79	-	-	-

[a] BET Surface area [b] Total Pore Volume at relative pressure (P/P_0) of 0.95 by single point method [c] Average Pore size [d] Periodicity of SBA-15 derived from a low angle XRD [e] Unit cell length [f] Pore wall thickness

The bimodal pore size distribution (Inset of Fig. 2) at higher ZrO_2 loading is due to the porous nature of SBA-15 and ZrO_2 respectively. The structural and textural characteristics of SBA-15, and ZrO_2/SBA-15 catalysts were presented in Table.1. The pore volume of catalysts decreases (from 0.96 cc/g for SBA-15 to 0.61 cc/g for 30ZS) with increase in ZrO_2 loading which is reflected in decrease in the values of surface area (from 703 $m^2 g^{-1}$ for SBA-15 to 429 $m^2 g^{-1}$ for 30ZS).

The morphological features of the catalysts were elucidated by means of scanning electron microscopy (SEM), Transmission electron microscopy (TEM) techniques. The images of the parent SBA-15, 25ZS catalysts were shown in Figure.3. The SEM images clearly indicate the presence of well ordered and hexagonal array of ordered structure of SBA-15 even after ZrO_2 impregnation[21,23]. In addition to these results, TEM images witness the arrangement of uniform hexagonal channels like a honey comb array[21-23]. TEM image of 25ZS (Figure.3 (d)) shows the presence of majority of ZrO_2 particles in highly dispersed state inside the pores of the SBA-15 and few ZrO_2 particles (in the form of patches) present outside of the pores of the SBA-15. The Pore channel width of SBA-15 and 25ZS appears to be same (~5.5 nm). The results from X-ray diffraction, N_2 physisorption, SEM and TEM, confirm the retention of mesoporous structure of SBA-15 even after ZrO_2 loading.

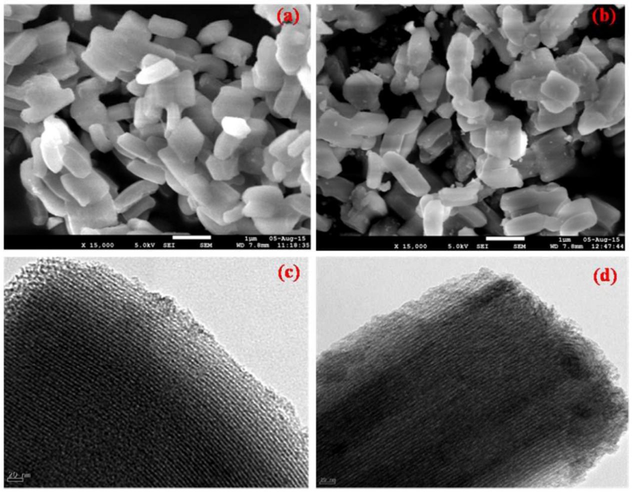

Fig. 3 SEM images of (a) parent SBA-15 and (b) 25ZS, TEM images of (c) parent SBA-15 and (d) 25ZS

Diffuse reflectance UV-Vis spectra of ZrO_2/SBA-15 catalysts and bulk ZrO_2 were shown in Figure. 4. The UV-DRS patterns of ZrO_2/SBA-15 catalysts show a broad absorption band around 205-215 nm due to the ligand-to-metal charge transfer (LMCT) from an O^{2-} to Zr^{4+} ion of highly dispersed Zr^{4+} in an isolated tetrahedral configuration[24,28] and a small band in the vicinity of ~230 nm was observed due to the presence of some bulk zirconia particles. Further a distinct absorption band at ~280 nm can be attributed to the well dispersed ZrO_2 nanoparticles[29-31]. These results confirm the presence of highly dispersed ZrO_2 species in ZrO_2/SBA-15 catalysts.

The ammonia desorption profiles of the SBA-15, ZrO_2/SBA-15 catalysts were depicted in Figure. 5 and the respective total acidity values were summarized in Table.2. The acidic sites population can be classified depending upon the desorption temperature of ammonia as weak acidic sites (<250 °C), medium (250-400 °C), and strong acidic sites (>400 C)[32,33]. The desorption signals observed in the TPD profile of pure SBA-15 can be ascribed to the surface hydroxyl groups[34,35].

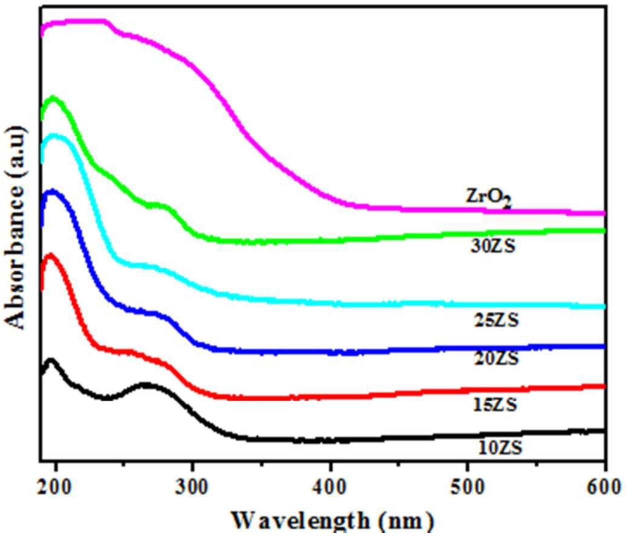

Fig. 4 UV-Vis-DRS spectra of ZrO_2 and various ZrO_2/SBA-15 catalysts

All the catalysts except SBA-15, showed a desorption peak in the temperature range of 130-250 °C indicating the weakly chemisorbed ammonia molecules corresponding to the presence of high amount of weak acidic sites arising from the dispersed zirconia. Another small peak at around 380 °C could be observed due to the presence of medium acidic sites. From the total acidity values (Table. 2) it can be observed that the acidity of the catalysts increases linearly with the zirconia loading.

Table.2 ZrO_2 loading and Acidity of ZrO_2/SBA-15 catalysts

Catalyst	Theoretical ZrO_2 Loading (wt %)	ZrO_2 loading by ICP (wt %)	Acidity (mmolNH_3/g)
SBA-15	0	0	0.17
10ZS	10	9.6	0.61
15ZS	15	13.2	0.80
20ZS	20	18.7	1.01
25ZS	25	23.1	1.49
30ZS	30	27.3	2.18

Thus ZrO_2/SBA-15 catalysts possess useful characteristics like larger surface area, dispersed acidic sites throughout the uniform pore channels for catalyzing the transfer hydrogenation and cyclization of LA under mild reaction conditions.

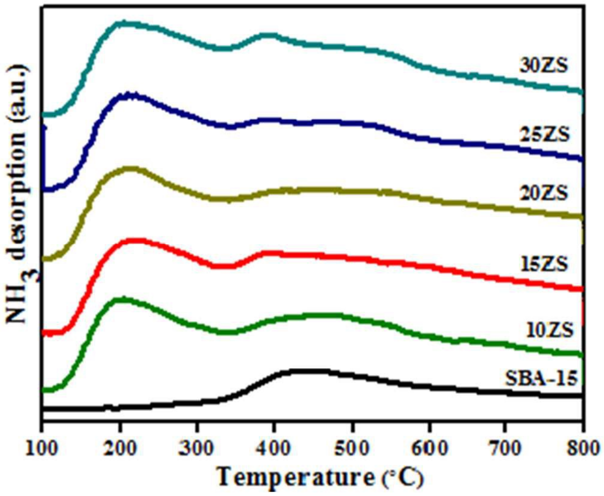

Fig. 5 NH_3-TPD profiles of parent SBA-15, and various ZrO_2/SBA-15 catalysts

3.1 Catalytic activity studies

3.1 Effect of ZrO2 loading

The effect of zirconia loading on the CTH of LA was studied in order to determine the optimum loading of zirconia, and the results were presented in Figure.6. The reaction path way was shown in Scheme. 1. The CTH of LA was tested with pristine SBA-15 and found the absence of GVL in the product mixture even though the LA conversion is 55%, suggesting the necessity of active species to catalyze the reaction. The reaction over pure zirconia shows 7 % selectivity to GVL with 96 % conversion of LA. The dispersion of zirconia on SBA-15 shows greater selectivity towards GVL due to not only the presence zirconia but also enhanced surface area and acidity

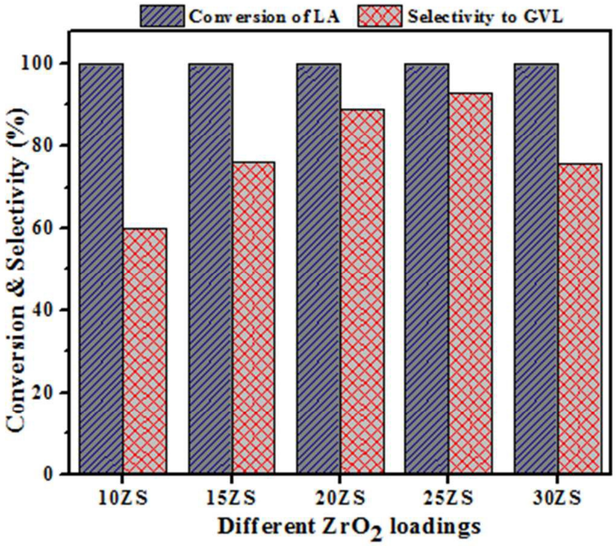

Fig. 6 Effect of ZrO_2 loading on CTH of levulinic acid with isopropanol Reaction conditions: Catalyst weight: 0.5g, LA:IPA=1:7 reaction temperature: 250 °C, N_2 flow: 30 ml/min, Liquid feed flow:1 ml/h

obtained through dispersion of zirconia over mesoporous silica SBA-15. The results show an increase in the selectivity towards GVL from 59 % to 93 % with increasing zirconia loading from 10 % to 25 % due to increase in the number of accessible zirconia active sites which are responsible for the transfer hydrogenation of and cyclization of LA. More number of acidic sites promotes the side reactions and therefore decrease in the selectivity to desired product is observed[36]. As the zirconia loading increases to 30 % decrease in selectivity towards the GVL is observed probably due to its higher acidity (as evidenced by NH_3-TPD Table.2) leading to the formation of dehydration products of the intermediate and ring opening products of GVL.

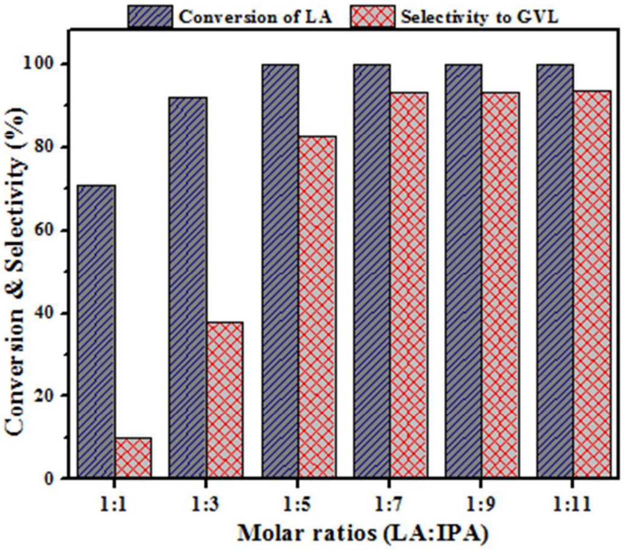

Fig. 7 Effect of IPA molar ratios on CTH of levulinic acid with isopropanol. Reaction conditions: Catalyst weight: 0.5g, reaction temperature: 250 °C, N_2 flow: 30 ml/min, Liquid feed flow: 1 ml/h

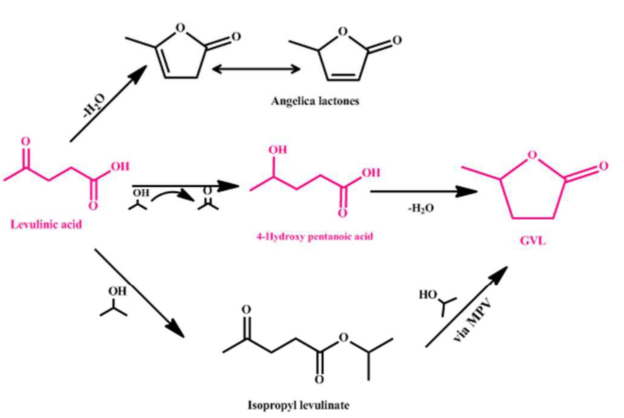

Scheme.1 Reaction pathway for the CTH of levulinic acid with isopropanol

3.2 Effect of molar ratio of isopropanol

The influence of the molar ratio of isopropanol (IPA) to LA to yield GVL was investigated on 25ZS catalyst and the results were illustrated in Figure-7. The selectivity towards GVL increases with increase in the molar ratio of IPA to LA and reaches a maximum selectivity of 93% at a molar ratio of 7. Because of the presence of keto and carboxylic acid functional groups in LA there is a competition between CTH and esterification reactions. At lower LA/IPA molar ratios of 1:1 and 1:3, the conversions of LA are 71 % and 92 % with selectivity's to GVL are 10% and 38% respectively. With increase in the molar ratio of IPA/LA to 5, LA conversion increases to 100% with 82% selectivity to GVL. Further increase in the molar ratio of IPA/LA to 7, maximum GVL selectivity of 93% was obtained. Further increase of IPA quantity results no considerable change in the selectivity to GVL. Hence it can be suggested that the maximum GVL selectivity can be achieved with IPA/LA molar ratio of 7.

3.3 Effect of temperature

The effect of temperature ranging from 250 °C (near to the boiling point of LA) to 310 °C on CTH reaction of LA was studied on 25ZS catalyst and the results were depicted in Figure. 8. The reaction performed at 230°C (lower than the boiling point of LA) exhibits 95% conversion of LA with 61% selectivity to GVL. The conversion of LA is 100% at all temperatures (250-310 °C), but the selectivity to GVL varies with temperature.

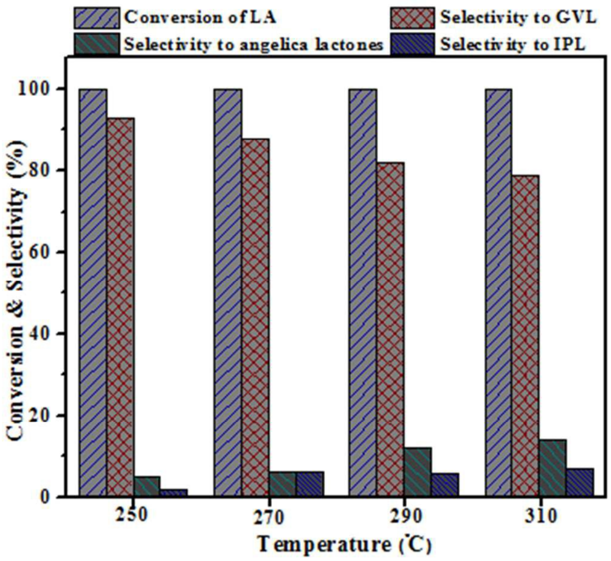

Fig.8 Effect of reaction temperature on CTH of levulinic acid with isopropanol Reaction conditions: Catalyst weight: 0.5g, LA: IPA =1:7, N_2 flow: 30 ml/min, Liquid feed flow: 1 ml/h

Diverse product distribution was witnessed as the temperature increases from 250 to 310 °C. The raise in temperature beyond 250 °C leads to the formation of angelica lactones through dehydration of LA, thereby decreasing the selectivity to GVL. These studies suggest that the optimum temperature for the CTH reaction is 250 °C

3.4 Time on stream studies

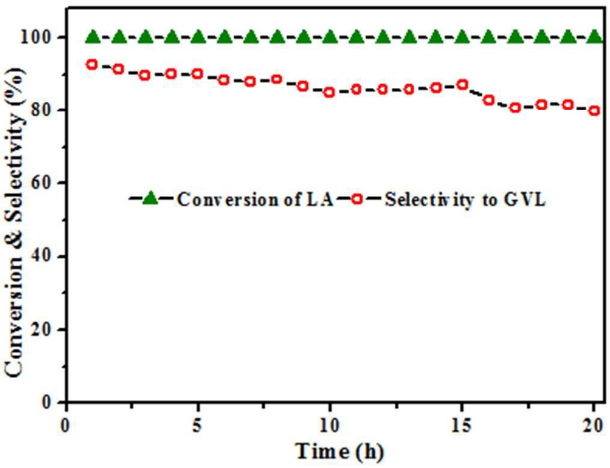

Fig.9 Influence of time on stream on CTH of levulinic acid with isopropanol Reaction conditions: Catalyst weight: 0.5g, LA: IPA =1:7 reaction temperature: 250 °C, N_2 flow: 30 ml/min, Liquid feed flow: 1 ml/h

The stability of the 25ZS catalyst was tested by performing the time on stream studies under the optimized reaction conditions. The results were presented in Figure. 9. The catalyst exhibits constant activity during 20 hours time on stream study. The conversion of LA remains at nearly 100% during the course of the reaction, while the selectivity to GVL decreases slightly. This may due to deposition of carbonaceous species formed by condensation products over the catalyst surface.

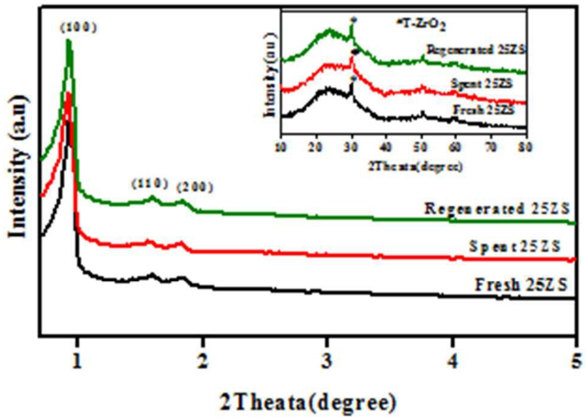

Fig. 10 Low angle and wide angle XRD patterns of 25ZS Catalysts

Interestingly, the catalyst displays (Figure. 12) similar catalytic activity after regeneration by calcining in air to remove the carbonaceous moiety. The spent and regenerated catalysts were characterized in order to know the reason for slight decline in the activity. The XRD patterns of the fresh, spent and regenerated catalyst were shown in Figure. 10. No change in the small angle and wide angle patterns indicates retainment of structure in 25ZS catalyst. The temperature programmed desorption of ammonia profiles of the three catalysts were presented in Figure.11 The total acidity of 25ZS fresh catalyst (1.49 mmol NH_3 g^{-1}) decreases to 0.90 mmol NH_3 g^{-1} after the reaction and regains to some extent (1.19 mmol NH_3 g^{-1}) after regeneration. TPD of ammonia profiles (Figure-11) clearly indicates that the decrease in the acidity is due to the depletion of weak and moderate acidic sites. It appears that the carbonaceous deposits occur on the weak and moderate sites. Further, the CHNS analysis shows the presence of carbon in the spent catalyst and absence of carbon in the regenerated catalyst. From these results, one can confirm that the deposition of carbonaceous species over the catalyst surface can decrease the catalytic activity slightly by blocking the active sites of the catalyst. The high activity and stability of the catalyst during time on stream study is due to the presence of ZrO_2 in highly dispersed form. ZrO_2 and other metal oxides can be presented in mesoporous silicas in various forms, like nano crystallites either inside or outside the pore channels or forming monolayer type species (mono- or polynuclear species formed by the reaction with surface silanol groups leading to reconstruction of inner walls of mesoporous channels[37].

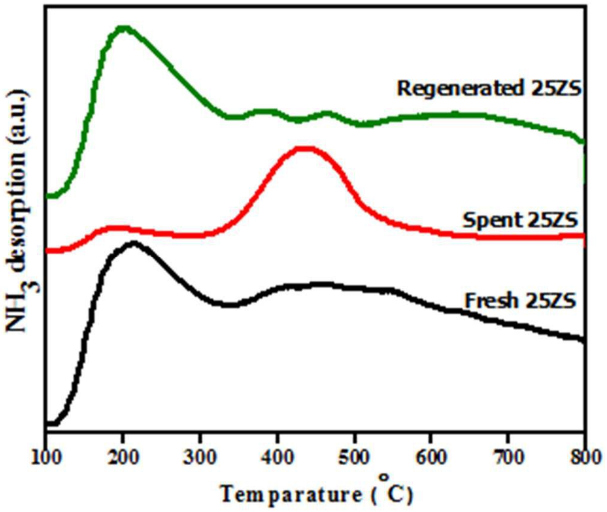

Fig. 11 TPD profiles of 25ZS catalysts

3.5 Influence of different alcohols and esters of LA

To explore the catalyst excellence, the CTH reaction of LA was conducted with different secondary alcohols under optimized reaction conditions and the results were depicted in Figure. 13. The conversion of LA is 100% with both 2-butanol, and cyclohexanol, besides that the selectivity to GVL is 96% and 91% respectively. Since the conversions of LA are 100% with IPA, 2-butanol, and cyclohexanol, the reactions were performed at higher feed flow rate. At a feed flow rate of

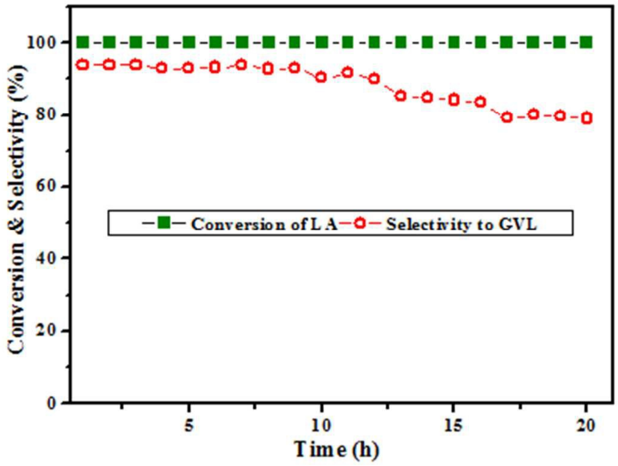

Fig. 12 Time on stream study of CTH of levulinic acid over regenerated 25ZS catalyst

Reaction conditions: Catalyst weight: 0.5g, LA: Alcohol =1:7 reaction temperature: 250 °C, N_2 flow: 30 ml/min, Liquid feed flow: 1 ml/h

3ml/h the conversions of LA with IPA, 2-butanol, and cyclohexanol are 95, 97 and 93% with selectivity to GVL are 72, 77 and 69% respectively. The selectivity to GVL is slightly higher with 2-butanol than with IPA. This is due to the lower reaction energies of the reaction between 2-butanol and LA[2].

Further, the catalytic performance of 25ZS catalyst was tested with methyl levulinate (ML) and ethyl levulinate (EL) instead of LA under optimized reaction conditions (results were presented in Figure. 14), as these are the by-products during the hydrolysis of cellulose and hemicelluloses. Even though the esters of levulinic acid, ML and EL are completely converted, selectivity's to GVL are 87% and 81% respectively. Since the conversions are 100%, the reactions were performed at high feed flow rate. At a feed flow rate of 3 ml/h over 25ZS catalyst, the conversions of LA, ML and EL are 96, 93 and 94% with selectivity's to GVL are 72, 66 and 63% respectively. The decrease in selectivity to GVL in case of ML and EL is due to the formation of dehydration products from the intermediate 4-hydroxy alkyl levulinate. The lactonization is easier in 4-hydroxy levulinic acid compared to 4-hydroxy alkyl levulinate having bulky alkyl groups[38].

Table.3. Comparison of 25ZS with reported catalysts

[a] EL is used instead of LA

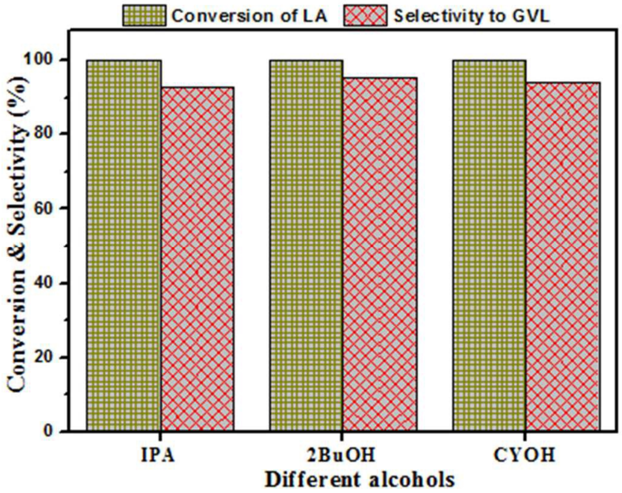

Fig. 13. Influence of various alcohols on CTH of levulinic acid Reaction conditions: Catalyst weight: 0.5g, LA: Alcohol =1:7 reaction temperature: 250 °C, N2 flow: 30 ml/min, Liquid feed flow: 1 ml/h

The catalytic performance of 25ZS catalyst was compared with other reported catalysts and summarized in Table.3.

The CTH of LA over pure zirconia exhibited lower selectivity to GVL (20-40%) at 20 bar pressure with high amount of 2-butanol[13]. In the CTH of EL over zirconia under supercritical conditions of ethanol (i.e. at 250 °C, 70 bar) the selectivity to GVL is 81.5% only[15]. Zr-beta zeolite exhibited good activity with high amount of IPA, but the catalyst preparation is complex[16]. Zr-HBA catalyst showed good activity in CTH of EL under batch conditions with excess amount of IPA[17]. Ni based catalysts were also found to be active for the titled reaction (79% LA conversion and 88% selectivity to GVL) at 10 bar pressure, with elevated amount of IPA[18].

7 weight % ZrO_2/SBA-15 catalyst showed 53% selectivity to GVL[23]. It is worth to mention that the present catalytic system offers the CTH of LA into GVL under vapour phase conditions with mild reaction conditions with low isopropanol quantity. These results pronounced the excellence of the 25ZS catalyst in the production of GVL in the absence of molecular hydrogen and harsh reaction conditions.

Catalyst	H_2 source	LA: H_2 source (Molar ratio)	Reaction conditions	LA conversion (%)	GVL selectivity /yield (%)	Ref.
ZrO_2	2-butanol	1:30	150 °C, 20 bar	100	20-40	13
[a]ZrO_2	Ethanol	1:49	250 °C, 70 bar	95.5	81.5	15
Zr-beta	2-propanol	1:37	150 °C, 1 bar	100	99	16
[a]Zr-beta	2-propanol	1:100	150 °C, 1 bar	100	94	17
Ni/MgO	2-propanol	1:66	150 °C, 10 bar	79	88	18b
7ZS	2-propanol	1:7	250°C, 1 atm	100	53	23
25ZS	2-propanol	1:7	250 °C, 1 atm	100	93	present

In addition, ZrO_2/SBA-15 catalysts were prepared by simple wet impregnation method. Other advantage associated with the present catalyst system is that there is no need of reduction step unlike in the metal catalysts[10].

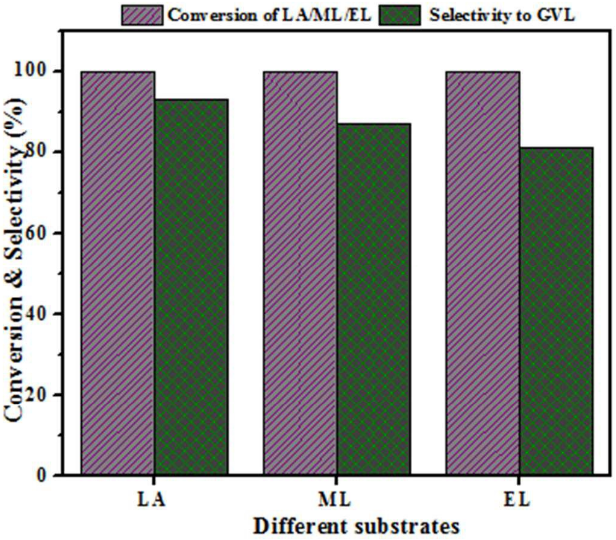

Fig. 14 Influence of levulinate esters on CTH with isopropanol Reaction conditions: Catalyst weight: 0.5g, EL/ML: IPA =1:7 reaction temperature: 250 °C, N_2 flow: 30 ml/min, Liquid feed flow: 1 ml/h

4. Conclusion

In conclusion, the ZrO_2/SBA-15 catalysts were successfully prepared by wet impregnation method without disturbing the mesoporous structure of SBA-15 and applied to the catalytic transfer hydrogenation and cyclization of LA to GVL with low quantity of H-donor (isopropanol) in a fixed bed down flow reactor at atmospheric pressure. The physicochemical characteristics of the catalysts were done systematically to know the structural, acidity and morphological features by means of XRD, temperature programmed desorption of ammonia, BET surface area, SEM, and TEM techniques. Under optimized reaction conditions 25ZS catalyst exhibited complete conversion of LA with 93% GVL selectivity. The superior catalytic performance of the 25ZS catalyst is attributed to presence of well dispersed acidic sites of ZrO_2 associated with improved surface area having sustained pore channels. The decrease in selectivity to GVL in case of ML and EL is due to the formation of the dehydration products from the intermediate, 4-hydroxy alkyl levulinate. The 25ZS catalyst effectively catalyzed the CTH of LA with different secondary alcohols as hydrogen donors. The constant catalytic activity with little drop in selectivity to GVL during 20 h time on stream studies specifies the robustness of the catalytic system. The slight decrease in selectivity towards GVL is due to the accumulation of carbonaceous species over the catalyst surface and thereby blocks the access to the active sites.

Acknowledgements

The authors E.S.S, G.V.R.B and K.M gratefully thank University Grant Commission, New Delhi, for financial support.

References

1 G.W. Huber, S. Iborra and A. Corma, *Chem. Rev*., 2006, **106,** 4044.
2 BP Statistical Review of World Energy, 2011.
3 N. Armaroli and V. Balzani, *Angew. Chem. Int. Ed.,* 2007, **46,** 52.
4 L. Bui, H. Luo, W.R. Gunther and Y. Romn-Leshkov, *Angew. Chem. Int.Ed.,* 2013, **52,** 8022.
5 G. W. Huber, J. N. Chheda, C. J. Barrett and J. A. Dumesic, *Science,* 2005, **308,** 1446.
6 J. J. Bozell, L. Moens, D. C. Elliott, Y. Wang, G. G. Neuenscwander, S. W.Fitzpatrick, R. J. Bilski and J. L. Jarnefeld, *Resour. Conserv. Recycl.,* 2000, **28,** 227; (b) B.V. Timokhin, V.A. Baransky and G.D. Eliseeva, Levulinic acid in organic synthesis. *Russian Chemical Reviews* 1999, **68(1)**, 73.
7 (a) K. Yan, C. Jarvis , J. Gu and Y. Yan, *Renewable and Sustainable Energy Reviews* 2015, **51,** 986; (b) R.H. Leonard, *Ind.Eng.Chem,* 1956, **48 (8),** 1330. (c) J. Zhang, S.B. Wu, B.Li, and H. D. Zhang, *ChemCatChem,* 2012, **4,** 1230
8 (a) I.T. Horvath, H. Mehdi, V. Fabos, L. Boda and L.T. Mika , *Green Chem.,* 2008, **10,** 238; (b) A. P. Dunlop and J. W. Madden, *US Patent*, 1957, **2786852;** (c) D.M. Alonso, S.G. Wettstein and J.A. Dumesic, *Green Chem.,* 2013, **15,** 584; (d) V. Fa bos, M.Y. Lui, Y. F. Mui, Y.Y. Wong, L.T. Mika, L. Qi, E. Csefalvay, V. Kovacs, T. Szucs and I.T. Horvath, *ACS Sustainable Chem. Eng,.* 2015, **3,** 1899.
9 K. Yan, Y. Yang, J. Chai and Y. Lu, *Appl. Catal. B*, 2015, **179,** 292.
10 (a) K. Yan, T. Lafleur, C. Jarvis and G. Wu, *J. Cleaner Prod.,* 2014, **72,** 230; (b) K. Yan, T. Lafleur, G. Wu, J. Liao, C. Ceng and X. Xie, *Appl. Catal. A*, 2013, **468,** 52; (c)P. P. Upare, J. M. Lee, D. W. Hwang, Shiva B. Halligudi, Y. K. Hwang and J. S. Chang *J. Ind. Eng. Chem.,* 2011, **17**, 287; (d) K.I. Shimizu, S. Kanno, K. Kon, Green Chem., 2014, **16,** 3899. (e) V. Mohan, C. Raghavendra, C.V. Pramod, B.D. Raju and K.S. Rama Rao, *RSC Adv.,* 2014, **4,** 9660;
11 R.S. Assary, L.A. Curtiss, and J. A. Dumesic, *ACS Catal.* 2013, **3,** 2694.
12 N. J. Wise, and J. M. J. Williams, *Tetrahedron Lett.* 2007, **48,** 3639.
13 M. Chia and J.A. Dumesic, *Chem. Commun.,* 2011, **47**, 12233.
14 X. Tang, H. Chen, L. Hu, W. Hao, Y. Sun, X. Zeng, L. Lin, S. Liu, *Applied Catalysis B: Environmental,* 2014, **147**, 827.
15 X. Tang, L. Hu, Y. Sun, G. Zhao, W. Hao and L. Lin, *RSC Advances,* 2013, **3,** 10277.
16 J. Wang, S. Jaenicke and G.K. Chuah, RSC *Adv.,* 2014, **4,** 13481.
17 J. Song, L. Wu, B. Zhou, H. Zhou, H. Fan, Y. Yang, Q. Meng and B. Han *Green Chem.,* 2015, **17**, 1626.
18 (a) Z. Yang, Y.B. Huang, Q.X. Guo and Y. Fu, *Chem. Commun.,* 2013, **49,** 5328; (b) J. Lv , Z. Rong , Y. Wang , J. Xiu, Y. Wang , and J. Qu ***RSC Adv.***, 2015,**5**, 72037.
19 Y. Zhu, S. Liu, S. Jaenicke, and G. Chuah, *Catalysis Today,* 2004, **97**, 249.
20 (a) G. Li, W.H. Fu, and Y.M. Wang, Catal.Commun.*,* 2015, **62,** 10; (b) J.F. Minambres, M. A. Aramendía, A. Marinas, J.M. Marinas and F.J. Urbano, *J. Mol.Catal. A,* 2011, **338,**121; (c) Y.

Zhu, S. Jaenicke and G.K. Chuah, *J. Catal.,* 2003, **218,** 396; (d) Y.Z. Zhu, G. Chuah and S. Jaenicke, *J. Catal*. 2004, **227,** 1.
21 D. Y. Zhao, J. L. Feng, Q. S. Huo, N. Melosh, G. H. Fredrickson, B. F. Chmelka and G. D. Stucky, *Science,* 1998, **279**, 548.
22 (a) S. Ganji, S.S. Enumula, R.K. Marella, K.S. Rama Rao and D.R. Burri, *Catal. Sci. Technol.,* 2014, **4**, 1813; (b) S. Ganji, P. Bukya, V. Vakati, K.S. Rama Rao and D.R. Burri, *Catal. Sci. Technol.,* 2013, **3**, 409; (c) A. Narani, R.K. Marella, P. Ramudu, K.S. Rama Rao and D.R. Burri, *RSC Adv.*, 2014, **4**, 3774; (d) G.M. Dhar, G.M. Kumaran, M. Kumar, K.S. Rawat, L.D. Sharma, B. David Raju, and K.S. Rama Rao, *Catal.Today,* 2005, **99**, 309; (e) V. Mohan, C.V. Pramod, M. Suresh, K. Hari Prasad Reddy, B. David Raju and K.S. Rama Rao, *Catal. Commun.,* 2012, **18** 89.
23 E.S. Sankar, V. Mohan, M. Suresh, G. Saidulu, B. David Raju and K.S. Rama Rao *Catal.Commun.,* 2016, **75**, 1-5.
24 S.Y. Chen, J.F. Lee and S. Cheng, *J.Catal.* 2010, **270**, 196.
25 J. Sauer, F. Marlow and F. Schuth, *Phys. Chem. Chem. Phys.,* 2001, **3,** 5579.
26 B. Katryniok, S. Paul, M. Capron, S. Royer, C. Lancelot, L.J. Duhamel, V.B. Baca, P. Rey and F. Dumeignil, *J. Mater. Chem.,* 2011, **21,** 8159.
27 S.W. King K., D. H Everett, R. A. W Haul, L Moscow, R.A.Pierotti, J Rouquerol and T Siemieniewska, *Pure Appl. Chem.,* 1985, ***57,*** 603.
28 M.S.Morey, G.D.Stucky, S.Schwarz and M.Froba, *J.Phys.Chem.B* 1999, **103,** 2037.
29 Q.Pan, A. Ramanathan, W. K. Snavely, R.V. Chaudhari and B. Subramaniam, *Ind. Eng.Chem. Res.* 2013, **52,** 15481.
30 A. Ramanathan, M.C.C. Villalobos, C. Kwakernaak, S. Telalovic and U. Hanefeld, *Chem. Eur. J.* 2008, **14,** 961.
31 J. El Haskouri, S. Cabrera, C. Guillem, J. Latorre, A. Beltran, D. Beltran , M.D. Marcos, and P. Amoros, *Chem. Mater.*, 2002, **14 (12**), 5015.
32 V. Mohan, V. Venkateshwarlu, C.V. Pramod, B.D. Raju, K.S. Rama Rao, *Catal. Sci. Technol.,* 2014, **4,** 1253.
33 A. Boreave, A. Auroux and C. Guimon, *Microporous Mater.,* 1997, **11,** 275.
34 P. Burattin, M. Che, and C. Louis, *J. Phys. Chem. B*, 1998, **102,** 2722.
35 M. Varkolu, V. Velpula, Saidulu Ganji, D.R. Burri, and S. R. R. Kamaraju, *RSC Adv.* 2015, **5**, 57201.
36 F.J. Urbano, M. A. Aramendía, A. Marinas, and J. M. Marinas, *J.Catal.,* 2009, **268,** 79.
37 K. Barbera , P. Lanzafame , A. Pistone , S. Millesi , G. Malandrino , A. Gulino , S. Perathoner and G. Centi, *J. Catal.,* 2015, **323**, 19.
38 A.M. Hengne and C.V. Rode, *Green Chem.,* 2012, **14,** 1064

Graphical abstract

ZrO_2/SBA-15 as an efficient catalyst for the production of γ-valerolactone from biomass derived levulinic acid in vapour phase at atmospheric pressure

Enumula Siva Sankar, G.V.Ramesh Babu, Kondeboina Murali, Burri David Raju, and Kamaraju Seetha Rama Rao*

Inorganic and Physical Chemistry Division, CSIR-Indian Institute of Chemical Technology, Hyderabad, India-5000071.

E-mail: ksramarao@iict.res.in & ksramarao.iict@gov.in

Fax: +91-40-27160921; Tel: +91-40-27193163.

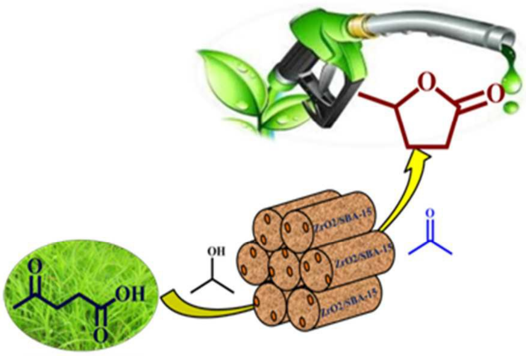

25 weight% ZrO_2 / SBA-15 catalyst exhibits good activity in the catalytic transfer hydrogenation of levulinic acid under vapour phase conditions at atmospheric pressure.